Parameter dependence of conic angle of nanofibres during electrospinning

Parameter dependence of conic angle of nanofibres during electrospinning

Zhengping Zhou[1]**, Xiang-Fa Wu**[1]**, Xueqin Gao**[2]**, Long Jiang**[1]**, Yong Zhao**[3] **and Hao Fong**[3]

[1] Department of Mechanical Engineering, North Dakota State University, Fargo, ND 58108, USA
[2] College of Polymer Science and Engineering, The State Key Laboratory of Polymer Materials Engineering, Sichuan University, Chengdu, Sichuan 610065, People's Republic of China
[3] Department of Chemistry, South Dakota School of Mines and Technology, Rapid City, SD 57701, USA

E-mail: Xiangfa.Wu@ndsu.edu (X-F Wu) and Hao.Fong@sdsmt.edu (H Fong)

Abstract

This paper reports the dependence of conic angle of nanofibres on the processing and material parameters during electrospinning. Solutions of polyacrylonitrile (PAN) in dimethylformamide (DMF) with varied PAN concentrations were studied as the model systems, and they were electrospun into nanofibres at different high direct current (dc) voltages, flow rates and needle diameters. The dynamic and transient shear viscosities of the PAN/DMF solutions were characterized by a parallel-plate rheometer at varied shear rates. Rheological measurements showed that the PAN/DMF solutions behaved as Newtonian fluids at relatively low to medium shear rates, while the solutions with high PAN concentrations of 18 and 20 wt% exhibited a significant shear-thinning behaviour at high shear rates, especially in the case of transient shear mode. Experimental results indicated that at the electrostatic field of $\sim 80\,\text{kV m}^{-1}$ and needle inner diameter of 0.48 mm (22 gauge), the conic angle of the nanofibre envelope decreased from $\sim 160°$ to $\sim 75°$ with an increase in PAN concentration from 12 to 20 wt%; at the PAN concentration of 16 wt%, the conic angle increased nonlinearly from $\sim 40°$ to $\sim 160°$ with an increase in electric field from 50 to $140\,\text{kV m}^{-1}$. In addition, experimental results showed that the needle inner diameter also noticeably influenced the conic angle. This study provided the experimental evidence useful for understanding the scaling properties of electrohydrodynamic jet motion for controllable electrospinning and process modelling.

(Some figures in this article are in colour only in the electronic version)

1. Introduction

The top-down nanofabrication technique of electrospinning is capable of producing fibres with diameters in the range from a few nanometres to micrometres (commonly known as 'electrospun nanofibres') [1–6]. To date, hundreds of natural and synthetic polymers as well as polymer-derived metals, carbon and ceramics have been electrospun into nanofibres with controlled fibre diameters and surface morphologies [7–12]. The family of electrospun nanofibres continues to expand with the growing research effort in this field. Due to the large surface-to-mass ratio (specific surface area), tailorable surface morphology, as well as relatively high degree of molecular orientation, electrospun nanofibres are suitable for uses in filtration, nanocomposite, wound dressing, tissue engineering, sensor/transistor, etc [7, 9–12]. In the recent years, the physical phenomena involved in the electrospinning process such as jet initiation, jet motion and destabilization, and nanofibre formation have been extensively studied under the endeavours particularly by Reneker and his co-workers [3, 4, 13–17] with the aid of high-speed imaging systems and theoretical modelling within the framework of electrohydrodynamics.

During a typical electrospinning process (e.g. that based on a polymer solution), a droplet forms at the spinneret (e.g. a capillary tube) of the electrospinning setup (see figure 1(a)) and deforms into a Taylor's cone under the action of electrostatic force [15, 18, 19]. When the electrostatic
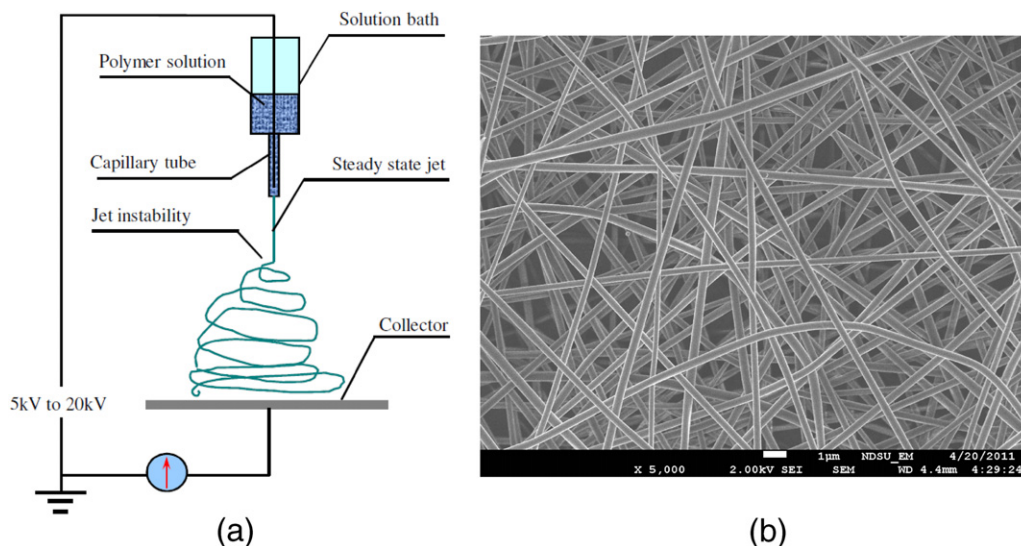
Figure 1. (*a*) Schematic setup of electrospinning and (*b*) SEM micrograph of PAN nanofibres produced by electrospinning a PAN/DMF solution with a PAN concentration of 13 wt%.

force overcomes the surface tension, a charged jet is ejected, which is then elongated in the electrostatic field. After a variety of jet destabilizations occurring simultaneously with solvent evaporation, the ultra-thinned jet is solidified and then deposited on the collector to form an overlaid nanofibre mat (see figure 1(*b*)). It is noteworthy that the process of electrospinning is very complicated, and it involves multiple physical phenomena such as electrohydrodynamics, diffusion and transfer of heat, solidification and crystallization, and the process has not yet been completely elucidated. The contemporary theoretical investigations are focused primarily on jet initiation [15, 18, 19], slender jet behaviour [20–28] and straight jet destabilization [13, 14, 20–23] as reviewed recently by Reneker *et al* [3]. Among these, to understand the whipping/bending instability of an electrospinning jet, Hohman *et al* [23] developed a linearized destabilization model to determine the critical condition of jet instability (i.e. the axisymmetric and asymmetric modes). This model has been used to predict the jet destabilization wavelength once the whipping/bending of a jet occurs, and has also been considered to correlate the final nanofibre diameter with the processing and material parameters [28]. In parallel, Reneker *et al* [13] formulated an efficient bead model to elucidate the whipping/bending instability of the jet in electrospinning. In this model, the jet is treated as a chain of beads (mass particles), each of which is connected through two neighbouring one-dimensional spring–dashpot elements based on the Maxwellian viscoelastic model with varying viscosity according to the extent of solvent evaporation. By further taking into account the effect of solvent evaporation, Yarin *et al* [14] refined this model to predict the jet trajectory at a distance up to 10 cm from the spinneret as largely validated by their experimental observations.

To date, numerous experimental and modelling studies have been carried out for understanding the fundamental electrohydrodynamic phenomena involved in the electrospinning process and the properties of the resulting nanofibres; these
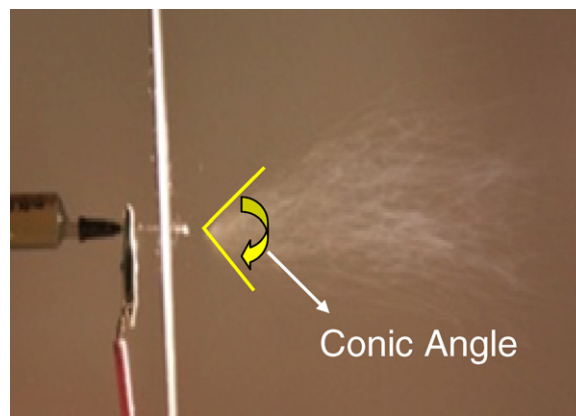

Figure 2. Formation of conic angle of nanofibre envelope during electrospinning of a PAN/DMF solution with a PAN concentration of 16 wt%.

include the recent studies on controllable nanofibre production, jet solidification and mechanical properties of electrospun nanofibres, among others [29–41]. The present experimental studies are targeted to further correlate the conic angle of nanofibre envelope (see figure 2) with the processing and material parameters employed in electrospinning including polymer concentration in the spinning solution, applied voltage, flow rate and needle diameter. The study of such correlations and parameters has not been systematic, although it is important to understand the fundamental phenomena of the electrospinning process, controllable nanofibre fabrication and the related process modelling. In this study, solutions of polyacrylonitrile (PAN) in dimethylformamide (DMF) with varied PAN concentrations were investigated as the model solutions for the preparation of electrospun nanofibres at different high direct current (dc) voltages, flow rates and needle inner diameters. The selection of PAN/DMF solutions is due to the fact that the PAN nanofibres are technically important, since they could be the precursor for further development of next generation carbon nanofibres with superior mechanical properties [42]. The

dynamic and transient shear viscosities of the PAN/DMF solutions were characterized within the typical range of electrospinnable PAN concentration using a parallel-plate rheometer at varied shear rates. The results acquired from this study can enrich the experimental database useful to controllable electrospinning and process modelling.

2. Experimental

The chemicals of PAN powder ($M_w = 150\,000\,\text{g mol}^{-1}$) and N, N-dimethylformamide (DMF, 99%) were purchased from the Sigma-Aldrich Co. (St Louis, MO). Nine PAN/DMF solutions with varied PAN concentrations in the range 12–20 wt% were prepared and used for electrospinning at different dc voltages. Prior to electrospinning, the PAN powder was dissolved in DMF using a magnetic stirrer installed with a hotplate; each mixture with different PAN concentrations was stirred at 80 °C for 6 h to prepare a well-electrospinnable solution. The dynamic and transient shear viscosities of the PAN/DMF solutions were characterized using a TA ARG2 Rheometer (TA Instruments, New Castle, DE) within the ranges of circular frequencies from 0.06 to 300 rad s^{-1} in the case of dynamic oscillating test mode and shear rates from 1 to 1000 s^{-1} in the case of transient shear test mode, respectively; the measured dynamic shear viscosity data are plotted in figure 3. During electrospinning, a PAN/DMF solution was placed in a 10 ml plastic syringe installed with a blunt-end stainless steel needle with the size of 20 gauge or 22 gauge (inner diameters: 0.48 mm for the 22-gaue needle and 0.65 mm for the 20-gauge needle), and the syringe was fixed onto a digitally controlled syringe pump (Fisher Scientific Inc., Pittsburgh, PA); two laboratory-made rectangular aluminium plates (51 cm × 31 cm) were placed in parallel with a distance of ~28 cm, of which one plate was electrically grounded and served as the nanofibre collector, and the other was isolated and used to generate a uniform electrostatic field in the space between the two plates. The latter was machined with an aperture allowing the needle tip of the syringe to pass through. Once a high dc voltage was applied between the needle and the grounded nanofibre collector through a positive high-voltage dc power supply (Gamma High Voltage Research, Inc., Ormond Beach, FL), a nearly uniform electrostatic field with dc voltage in the range 0–30 kV was established. The flow rate of the solution was varied to study its influence on the conic angle of the nanofibre envelope. Once a stable conic angle was formed under certain processing and material parameters, the nanofibre envelope was captured using a digital camera. The conic angles were then measured digitally from the images of the nanofibre envelopes and are tabulated in tables 1 and 2 and plotted in figures 4 and 5.

3. Results and discussion

Figure 3 shows the dynamic and transient shear viscosities of the PAN/DMF solutions as a function of shear rate for five typical PAN concentrations. At a given shear rate in the case of either dynamic oscillating test mode or transient shear test mode, the experimental viscosity increases with an
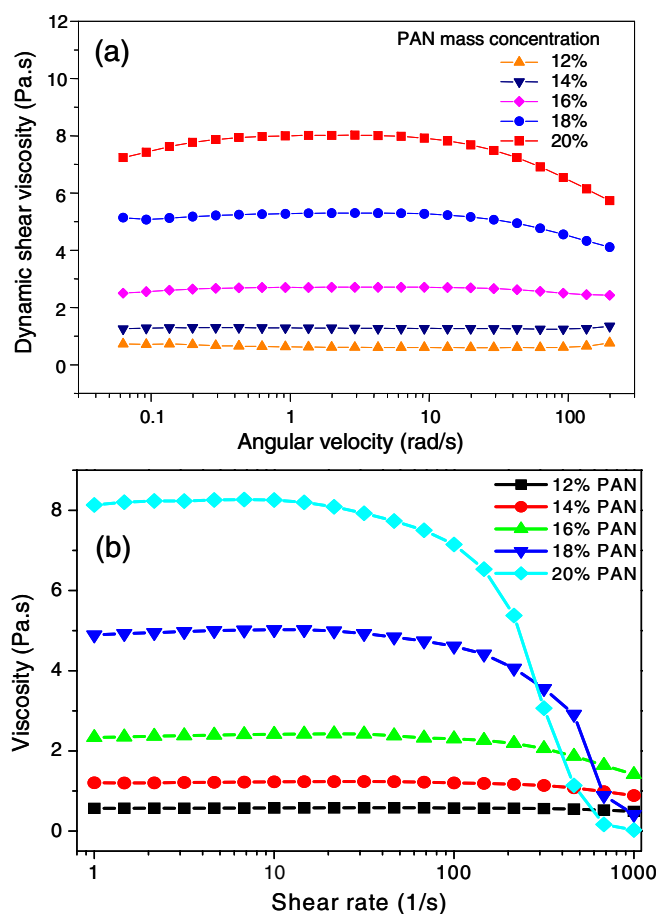

Figure 3. Variation of dynamic and transient shear viscosities with varying angular velocity and shear rate for PAN/DMF solutions at different PAN concentrations.

increase in PAN concentration as commonly observed in other systems of polymer solutions. At a fixed PAN concentration, the dynamic or transient shear viscosity is almost a constant at relatively low PAN concentrations (e.g. 12%, 14% and 16%), while both viscosities decrease with an increase in shear rate at high PAN concentrations (e.g. 18% and 20%). In particular, when the shear rate is higher than $100\,\text{s}^{-1}$, the transient shear viscosity of the solutions with PAN concentrations of 18% and 20% decreases significantly and is even lower than those of the solutions with low PAN concentrations, as shown in figure 3(*b*). This phenomenon was mainly induced due to the shear-thinning effect typically observed in polymer solutions at a high shear rate [43]. In this case, the macromolecular chains are aligned and have no sufficient time to relax. Even though the liquid of electrospinning jet was under extensional stretching, the measured dynamic or transient shear viscosity could be justified to qualitatively estimate the dynamic extensional viscosity via the positive correlation between the two viscosities [44]. One conclusion that can be drawn from the rheological measurements is that highly aligned molecular chains in polymer nanofibres can be achieved through spinning high-concentration polymer solutions (even polymer melts) at a high transient drawing rate.

Figure 4 shows that, for the PAN/DMF solution at a fixed PAN concentration of 16 wt% with a fixed flow rate

Table 1. Experimental measurements on the variation of conic angle for electrospinning PAN/DMF solutions (16 wt%) under varied electric field (needle inner diameter: 0.48 mm).
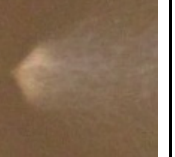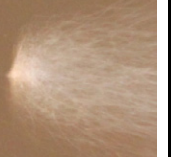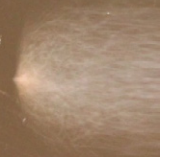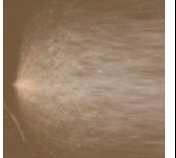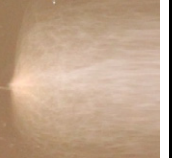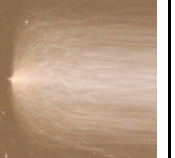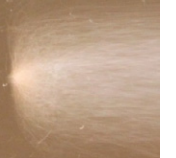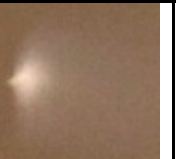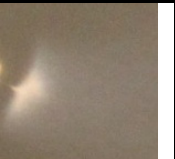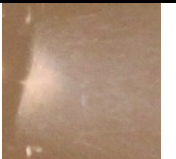
Electric Field (kV/m)	50	60	70	80	90
Images					
Conic angle (°)	36.3	84.1	107.1	135	150.5
Electric Field (kV/m)	100	150	120	130	140
Images					
Conic angle (°)	155.8	154.7	161.6	163.4	160.8

Table 2. Experimental measurements on the variation of conic angle for electrospinning PAN/DMF solutions at different PAN concentrations (wt%) under a constant electric field of $80 \, \text{kV m}^{-1}$ (needle inner diameter: 0.48 mm).

PAN concentration (wt. %)	12	13	14	15	16
Images					
Conic angle (°)	158.6	164.8	165.7	155.8	135
PAN (wt. %)	17	18	19	20	
Images					
Conic angle (°)	116.1	106.5	91.2	71.3	

of $0.6 \, \text{ml h}^{-1}$, the conic angle increases nonlinearly with the increase in dc voltage. When installed with a needle of inner diameter 0.48 mm (22-gauge needle), the measured conic angle is from $\sim 36.3°$ at the electric field of $\sim 50 \, \text{kV m}^{-1}$ to $\sim 160°$ at the electric field of $140 \, \text{kV m}^{-1}$ (table 1). In contrast, when installed with a large-sized needle of inner diameter 0.65 mm (20-gauge needle), the conic angle first increases with an increase in electric field until $90 \, \text{kV m}^{-1}$ and then decreases with a further increase in electric field. This could be induced due to the fact that with large spinning area (i.e. cross-sectional area of the needle) and fixed flow rate, the electrohydrodynamic behaviour of a jet varies on enlarging the drawing force to a critical value (i.e. a high electric field) due to the variation of Taylor's cone; i.e. the jet becomes under insufficient flow supply at high electric fields.

In general, charges induced on an electrospinning jet increase with the increase in electric field. From the images listed in table 1, it can be concluded that a higher dc voltage

enhanced the electrostatic shielding effect of the charged whipping/bending jet, leading to a larger conic angle. To estimate the magnitude of axial electrostatic stress of a whipping/bending jet, as a simplified approach, consider a liquid torus with evenly distributed surface charge Q, torus radius r, and the axisymmetric axis of the torus parallel to the electrostatic field. Coulomb's law determines the axial electrostatic stress of the jet, $\sigma = Q^2/(4\pi \varepsilon_a V_0 r)$, where ε_a is the dielectric constant of air, V_0 is the volume of the torus, and this stress decreases with an increase in torus radius r. The difference between the electrostatic stress and the jet viscoelastic stress is the driving stress to stretch/thin the jet. Interestingly, this simple estimate shows that the axial electrostatic stress is independent of the jet cross-sectional area. In reality, the dynamic extensional viscosity of the liquid in the jet grows rapidly with solvent evaporation. Thus, it can be expected that vigorous jet stretching would occur at the beginning of jet whipping/bending, where both the torus radius r and the jet viscosity are low, and significantly decay
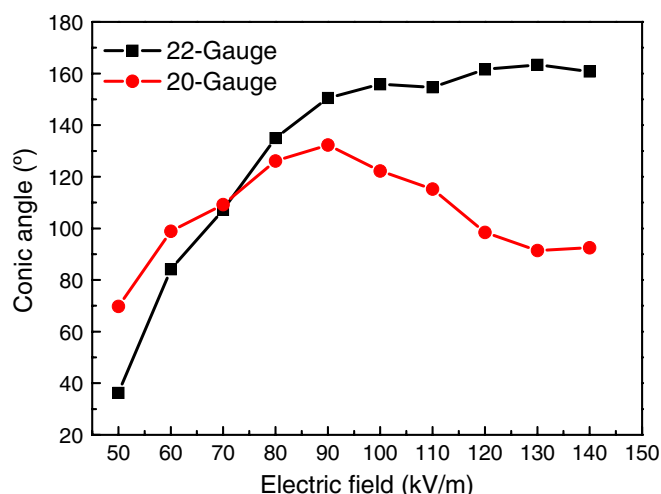
J. Phys. D: Appl. Phys. **44** (2011) 435401

Z Zhou *et al*

Figure 4. Experimental measurements on the variation of conic angle formed by PAN nanofibres with varying electric field (kV m^{-1}) at a constant PAN concentration of 16 wt% and two needle inner diameters (20 gauge and 22 gauge, respectively).
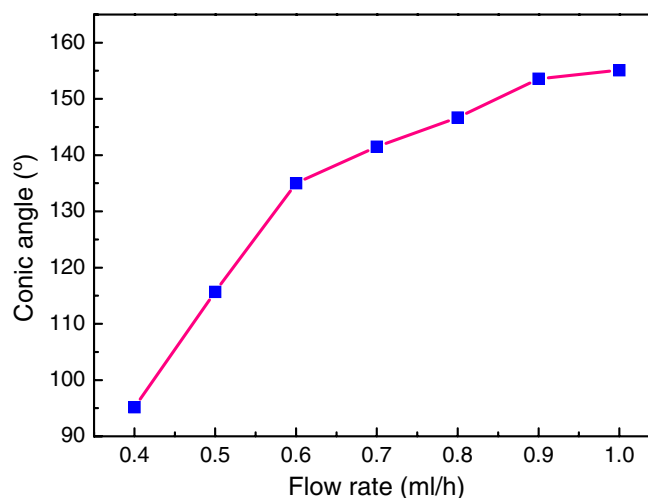

Figure 6. Experimental measurements on the variation of conic angle formed by PAN nanofibres with varying flow rate at a constant PAN concentration of 16 wt% and electric field of 80 kV m^{-1} (needle diameter: 0.48 mm).

is still desired to correlate the conic angle with the processing and material parameters.

Finally, to investigate the effect of flow rate on the conic angle, the electrospinning was performed at the PAN concentration of 16 wt%, applied electric field of 80 kV m^{-1} and needle inner diameter of 0.48 mm (22-gauge needle). Figure 6 shows the variation of the conic angle with respect to the flow rate in the range 0.4–1.0 ml h^{-1}. The experimental measurements show that the conic angle increases from 95° at the flow rate 0.4 ml h^{-1} to 155° at the flow rate 1.0 ml h^{-1}. Therefore, the flow rate has a significant effect on the conic angle. Such an effect is mainly due to the formation of a varying Taylor's cone in the electrospinning process when the flow rate is changed. Typically, a large flow rate corresponds to a large droplet at the needle outlet, which alters the jet initiation (e.g. the initial jet diameter, jet velocity, etc) and finally the conic angle of the nanofibre envelope.
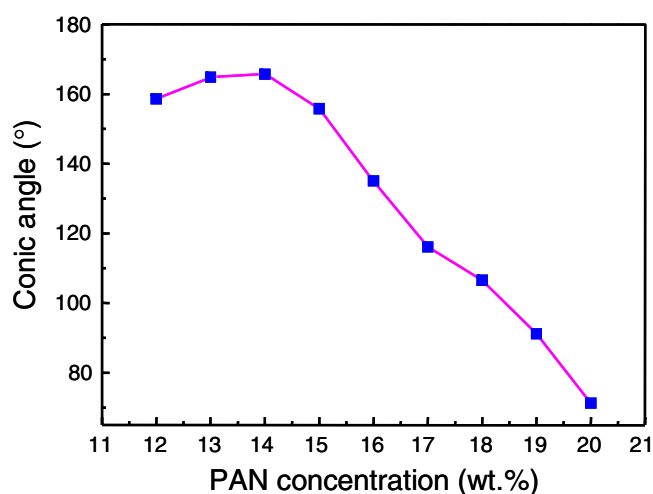

Figure 5. Experimental measurements on the variation of conic angle formed by PAN nanofibres with varying PAN concentration (wt%) at a constant electric field of 80 kV m^{-1} (needle diameter: 0.48 mm).

4. Concluding remarks

In summary, a detailed experimental investigation is carried out to explore the dependence of the conic angle of a nanofibre envelope on the polymer concentration, applied dc voltage, flow rate and needle inner diameter employed in electrospinning. The experimental results provide an insight into the fundamental electrohydrodynamic phenomenon in the electrospinning process, which can facilitate the research on controllable fabrication of electrospun nanofibres for numerous applications as well as relevant process modelling.

with solvent evaporation. This was validated by experimental observations using the high-speed imaging technique. A more detailed phenomenological description based on the discrete-bead models [13, 14] gave similar conclusions.

Furthermore, at a given electric field (∼80 kV m^{-1}), the experimentally observed conic angle of the nanofibre envelope decreases nonlinearly with the increase in PAN concentration from ∼160° at 12 wt% to ∼71° at 20 wt%, as shown in table 2 and figure 5 (with 22-gauge needle). In this case, the PAN/DMF solution with a low PAN concentration corresponds to a low viscosity. This means that the jet can be easily stretched under electrostatic interaction of the induced charges, i.e. a large conic angle can be detected accordingly. Although recent theoretical models [13, 14] can predict the initial conic angle to some extent with simplified electrostatic interactions based on a limited number of beads, a generalized scaling law

References

[1] Reneker D H and Chun I 1996 *Nanotechnology* **7** 216
[2] Doshi J and Reneker D H 1995 *J. Electrostatics* **35** 151
[3] Reneker D H, Yarin A L, Zussman E and Xu H 2007 *Adv. Appl. Mech.* **41** 43
[4] Reneker D H and Yarin A L 2008 *Polymer* **49** 2387
[5] Dzenis Y 2004 *Science* **304** 1917

[6] Rutledge G C and Fridrikh S V 2007 *Adv. Drug Deliv. Rev.* **59** 1384

[7] Huang Z M, Zhang Y Z, Kotaki M and Ramakrishna S 2003 *Compos. Sci. Technol.* **63** 2223

[8] Li D and Xia Y N 2004 *Adv. Mater.* **16** 1151

[9] Greiner A and Wendorff J H 2007 *Angew. Chem. Int. Edn* **46** 5670

[10] Ramakishna R, Sundarrajan S, Jose R and Ramakrishna S 2007 *J. Appl. Phys.* **102** 111101

[11] Ramakishna S, Fujihara K, Teo W E, Lim T C and Ma Z 2005 *An Introduction to Electrospinning and Nanofibers* (Singapore: World Scientific)

[12] Andrady A L 2008 *Science and Technology of Polymer Nanofibers* (New York: Wiley)

[13] Reneker D H, Yarin A L, Fong H and Koombhongse S 2000 *J. Appl. Phys.* **87** 4531

[14] Yarin A L, Koombhongse S and Reneker D H 2001 *J. Appl. Phys.* **89** 3018

[15] Yarin A L, Koombhongse S and Reneker D H 2001 *J. Appl. Phys.* **90** 4836

[16] Yarin A L, Kataphinan W and Reneker D H 2005 *J. Appl. Phys.* **98** 064501

[17] Reneker D H and Fong H (ed) 2005 *Polymeric Nanofibers* (Washington, DC: American Chemical Society)

[18] Taylor G 1969 *Proc. R. Soc. Lond.* A **313** 453–75

[19] Spivak A F and Dzenis Y A 1999 *J. Appl. Mech.* **66** 1026

[20] Kirichenko V N, Petryanov-Sokolov I V, Suprun N N and Shutov A A 1986 *Sov. Phys.—Dokl.* **31** 611

[21] Spivak A F and Dzenis Y A 1998 *Appl. Phys. Lett.* **73** 306

[22] Spivak A F, Dzenis Y A and Reneker D H 2000 *Mech. Res. Commun.* **27** 37

[23] Hohman M M, Shin M, Rutledge G and Brenner M P 2001 *Phys. Fluids* **13** 2201

[24] Hohman M M, Shin M, Rutledge G and Brenner M P 2001 *Phys. Fluids* **13** 2221

[25] Shin Y M, Hohman M M, Brenner M P and Rutledge G C 2001 *Appl. Phys. Lett.* **78** 1149

[26] Feng J J 2002 *Phys. Fluids* **14** 3912

[27] Feng J J 2003 *J. Non-Newtonian Fluid Mech.* **116** 55

[28] Fridrikh S V, Yu J H, Brenner M P and Rutledge G C 2003 *Phys. Rev. Lett.* **90** 144502

[29] Theron S A, Zussman E and Yarin A L 2004 *Polymer* **45** 2017

[30] Thompson C J, Chase G G, Yarin A L and Reneker D H 2007 *Polymer* **48** 6913

[31] Tripatanasuwan S, Zhong Z X and Reneker D H 2007 *Polymer* **48** 5742

[32] Wu X F, Salkovskily Y and Dzenis Y A 2011 *Appl. Phys. Lett.* **98** 223108

[33] Zussman E, Rittel D and Yarin A L 2003 *Appl. Phys. Lett.* **82** 3958

[34] Wu X F and Dzenis Y A 2007 *J. Appl. Phys.* **102** 044306

[35] Wu X F and Dzenis Y A 2007 *J. Phys. D: Appl. Phys.* **40** 4276

[36] Wu X F and Dzenis Y A 2007 *Nanotechnology* **18** 285702

[37] Naraghi M, Chasiotis I, Kahn H, Wen Y and Dzenis Y 2007 *Appl. Phys. Lett.* **91** 151901

[38] Wu X F, Kostogorova-Beller Y Y, Goponenko A V, Hou H Q and Dzenis Y A 2008 *Phys. Rev.* E **78** 061804

[39] Lim C T, Tan E P S and Ng S Y 2008 *Appl. Phys. Lett.* **92** 141908

[40] Wu X F, Bedarkar A and Akhatov I S 2010 *J. Appl. Phys.* **108** 083518

[41] Wu X F 2010 *J. Appl. Phys.* **107** 013509

[42] Liu J, Yue Z and Fong H 2009 *Small* **5** 536

[43] Bird R B, Armstrong R C and Hassager O 1987 *Dynamics of Polymeric Liquids* vol 1 *Fluid Dynamics* 2nd edn (New York: Wiley Inter-Science)

[44] Barnes H A and Roberts G P 1992 *J. Non-Newtonian Fluid Mech.* **44** 113